Maintenance of the Arctic Ocean large-scale baroclinic structure by the M2 tide

IGOR V POLYAKOV

Polyakov, Igor V. 1995 00 00: Maintenance of the Arctic Ocean large-scale baroclinic structure by the M2, tide

A three-dimensional structure of the M2 tidal currents has been reproduced by mathematical modelling. The possibility of energy transfer from the tidal barotropic motion to large-scale baroclinic circulation of the Arctic Ocean has been estimated. It has been shown that the bottom relief plays an important role in the formation of the large-scale pattern of the baroclinic fields. The hypothesis has been proposed that the M2 tide may support the near-slope convection of the East-Siberian and Laptev seas. *Polar Research 13(2)*, 219–232

Igor V. Polyakov, Arctic & Antarctic Research Institute, 38 Bering st., St. Petersburg 199397, Russia.

Introduction

The objective of this study is to estimate the influence of the Arctic Ocean M2 tide on the formation of the ocean's density and velocity fields.

The study of the Arctic Ocean tides has a long history. In 1924, Defant showed that the Arctic Ocean semi-diurnal tides are caused by the tidal wave spreading from the Atlantic Ocean, and that diurnal tides are formed in the Arctic. Later, several studies have appeared where the tidal dynamics of the Arctic Ocean both as a separate basin (Gjevik & Straume 1989; Kowalik 1981; Kowalik & Proshutinsky 1993; Kowalik & Untersteiner 1978; Proshutinsky 1993) and as a part of the World Ocean (Hendershott 1977; Schwiderski 1980 and others) has been investigated. For various reasons the authors of the mentioned studies took into account the two-dimensional structure of the tides in the barotropic ocean only.

One of the first attempts to investigate the tides in a baroclinic ocean was a paper by Kagan (1968). Using some assumptions, Kagan analytically obtained relations for the calculation of the sea water level, density and three components of the velocity vector in the tidal flow. The influence of the sea water stratification on the tidal dynamics by a dimensionless parameter has been estimated. It was shown that the tidal surface elevation and currents in a baroclinic ocean differ insignificantly from that in the stratified ocean.

Several models of tidal dynamics in a stratified two-dimensional channel (x-z axes) have been developed (Blumberg 1976; Hamilton 1976; Johns 1975; Johns 1978). On the one hand, such models have been an excellent proving ground for the development of three-dimensional (3D) baroclinic models. On the other hand, these models have provided quite realistic results for tidal dynamics in narrow channels.

In 1976, Caponi simulated wind-driven and tidal circulation and salt redistribution in the Chesapeake Bay using a 3D baroclinic model. He had significant limitations in computer resources, and poor resolution and low order accuracy schemes resulted in very weak tidal variations in the salinity field.

The application of a 3D baroclinic model by Leendertse & Liu (1977) to the San-Francisco Bay and the Alaskan shelf has also been limited by inadequate computer resources. However the authors have later simulated the circulation and baroclinic fields transformation under the joint effect of the wind, tide and fluxes through the open boundaries in the Bristol Bay (Liu & Leendertse 1979) and on the Alaskan shelf (Liu & Leendertse 1987). Leendertse and Liu estimated the influence of stratification on the tidal dynamics.

Oey et al. (1985) carried out numerical experiments in the reconstruction of the circulation and baroclinic processes in the Hudson Estuary from July to September 1980. They used a 3D time-dependent baroclinic model (Blumberg & Mellor 1983) with free surface. The forces were the tidal wave spreading in the basin from the Atlantic Ocean, the wind stresses, river inflow, and the

salinity gradients. Because of the high resolution, the model produced eddies. As Blumberg and Mellor had supposed, the interaction of the density and velocity with the bottom relief caused small eddies (3 km × 3 km × 10 m) which moved and were transformed in time. According to Blumberg and Mellor's published conclusions, along with the baroclinic instability, this mechanism was considered as the most important process in the estuary.

Numerical modelling was the method employed in this study. Our experiments had two stages. The first was a simulation of the level oscillations and 3D currents produced by the M2 tidal wave penetrating into the barotropic Arctic Ocean from the Atlantic Ocean. The comparison of the calculated and observed sea level data was carried out to validate the model results. Unfortunately, we have only been able to use sea level observation data. Further, we have simulated the M2 tidal dynamics in the stratified Arctic Ocean. However the objective of the experiment was not only to reproduce the tide in the baroclinic ocean but also to estimate the possible changes in the Arctic Ocean baroclinic fields caused by periodical forcing. For this purpose the system with initial horizontally homogeneous salinity was adopted and there were no salt sinks and sources throughout all the basin boundaries during the experiment. Due to small temperature-induced density variations in the Arctic Ocean (Aagaard & Carmack 1989), we have neglected the temperature variability.

Model description

The non-linear primitive momentum equations with the Boussinesq approximation, the heat and salt balance equations, the hydrostatic and continuity equations, and the equation of state are the following

$$\partial\bar{U}/\partial t + (\bar{V}\nabla)\bar{U} + f\bar{k} \times \bar{U} = -\rho_0^{-1}\nabla_H P + \bar{F}; \quad (1)$$

$$\partial P/\partial t = \rho g; \quad (2)$$

$$\partial W/\partial z = -div_H\bar{U}; \quad (3)$$

$$\partial(T,S)/\partial t + L(T,S) = \partial[(\upsilon_H,\upsilon_s)\partial(T,S)/\partial z]/\partial z + A_{HH}\nabla_H^2(T,S) + \delta_c(T,S); \quad (4)$$

$$\rho = \rho(T,S,P); \quad (5)$$

where the advective operator L is defined by

$$Lq = \partial(Uq)/\partial x + \partial(Vq)/\partial y + \partial(Wq)/\partial z; \quad (6)$$

q represents any scalar value, diffusive operator $\bar{F}$ has the following form

$$\bar{F} = (F_X,F_Y) = [\partial(\upsilon_0 + \upsilon_M)\partial/\partial z/\partial z + A_{MH}\nabla_H^2](U,V); \quad (7)$$

A convective mechanism is described by the term δc (T,S) (Bryan 1969) and means the vertical weight averaging of the temperature and salinity when the density instability occurs. z is the vertical axis directed vertically down to the bottom from the ocean surface. The symbols used here denote: $\bar{V} = (\bar{U},W) = (U,V,W)$ is the velocity vector, W is the vertical velocity component; T is potential temperature; S is salinity; $\bar{k}$ is the unit vector parallel to the z-axis, $f = 2\,\omega Sin\,\varphi$, $\omega = 7.29 \times 10^{-5}$ rad/sec is the Earth rotation rate, φ is latitude; ρ is density; ρ_0 is a reference density; P is pressure; g is the acceleration of gravity; A_{MH},A_{HH},υ_M,υ_H,υ_S are eddy diffusivity coefficients of momentum, heat and salt exchange in the horizontal and vertical directions, respectively; $\upsilon_0 = 0.1\,cm^2/s$ is the molecular viscosity coefficient; $\nabla H = (\partial/\partial x, \partial/\partial y)$; ∇^2 is the horizontal Laplacian operator and div_H is the horizontal divergence vector. The equation of state (5) is written in the Eckart's form (Semtner 1974).

In the experiment the temperature variations have been neglected. That seems to be not an excessive assumption as the Arctic Ocean thermohaline variability is primarily determined by the salinity (Aagaard & Carmack 1989). Therefore we have used only one equation (4) for the salinity. That has enabled us to reduce the calculation time significantly.

The vertical velocity W at the top $z = \xi$ and at the bottom z = H is written respectively

$$W = -\partial\xi/\partial t - \bar{U}\nabla_H\xi; \quad (8)$$

$$W = -\bar{U}\nabla_H H. \quad (9)$$

Here ζ(x,y,t) is the surface level elevation. For easy reading of the figures we assume that the positive direction of the level deviation is opposite to the z-axis.

To reduce the time of calculations we use the splitting procedure when the velocity is presented as a sum of 'baroclinic' and 'barotropic' components (Killworth et al., 1987). We shall determine the horizontal components of the velocity

vector as a sum

$$\bar{U} = \bar{M}/H + \bar{U}'. \tag{10}$$

where $\bar{M} = (M_X, M_Y)$ are vertically integrated mass fluxes

$$\bar{M} = \int_{\xi}^{H} \bar{U} dz, \tag{11}$$

and $\bar{U}' = (U', V')$ is the baroclinic velocity with zero vertically mean value which is computed by the equation (1).

Taking into account the kinematic boundary conditions (8) and (9) we shall integrate the equations (1) and (3) from ξ to H with respect to z. With consideration of (8) we obtain

$$\partial\xi/\partial t + div_H \bar{M} = 0; \tag{12}$$

$$\partial\bar{M}/\partial t + f\bar{k} \times \bar{M} = -gH\nabla_H \xi + A_{MH} H \nabla_H^2 (\bar{M}/H) + \rho_0^{-1}(\tau^S - \tau^B) - L \int_{\xi}^{H} \bar{U} dz - g\rho_0^{-1} \times \int_{\xi}^{H} \left(\int_{\xi}^{z} \nabla_H \rho dz' \right) dz. \tag{13}$$

Here τ^B is the bottom stress vector, which is determined by a quadratic law on the mass flux $\bar{M}$ with 0.0026 drag coefficient; the wind stress vector τ^S in these experiments was equal to zero.

Finally, the vector $\bar{U} = (U,V)$ is obtained by the relation (10) (Bryan 1969; Killworth et al. 1987).

According to Prandtl, the coefficient υM is described by the expression (Voltsinger et al. 1989):

$$\upsilon_M = l^2 |\partial\bar{U}/\partial z|. \tag{14}$$

Prandtl's formula follows from the equation of turbulent energy balance if we keep only the terms of energy generation by velocities shear and dissipation.

To calculate a turbulent scale l in (14) the following expression has been suggested

$$l = \kappa H^{-1} Z_\xi Z_H Z_0, \tag{15}$$

where $k = 0.4$ is the von Karman constant; $Z_H = H - z + z_H$; $Z_\xi = z + z_\xi - \xi$; $z_H = z_\xi = 2.5$ cm are the parameters of roughness near the bottom and surface (Voltsinger et al. 1989). Z_H and Z_ξ allow allocation of two boundary layers. We use $Z_0 = (1 - \beta H^{-2} Z_H Z_\xi)/(H/H_0 + 1)$ ($H_0 = 25$ m,

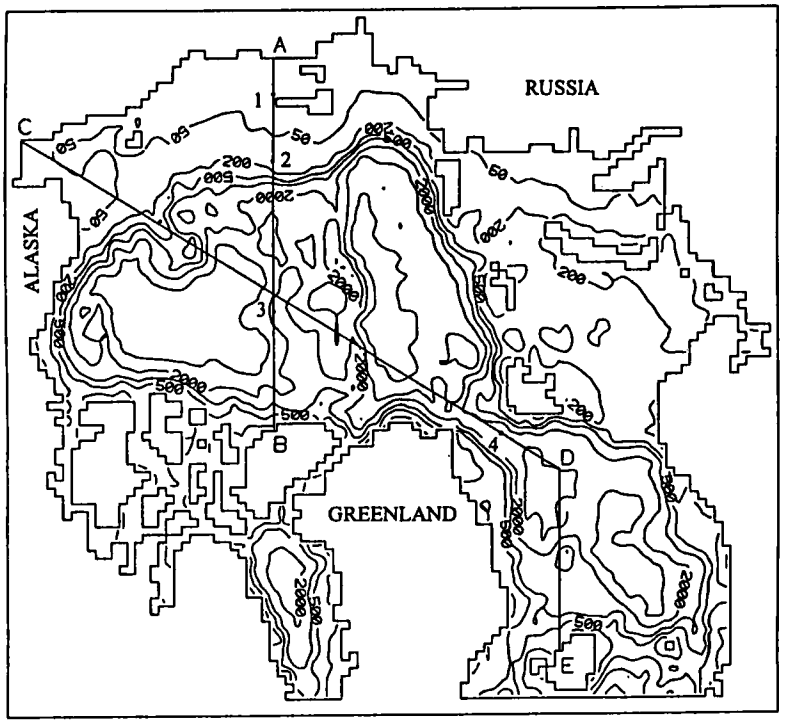

Fig. 1. Model domain of the Arctic Ocean. Depth contours are in metres. AB and CDE are the lines of vertical cross-sections. The numbers 1, 2, 3, 4 denote points where the vertical salinity profiles have been presented. One grid step is equal to 55.6 km.

$\beta = 1.2$ is an empirical constant) to apply this parameterisation to the deep ocean. The z-axis model formulation is restricted so that the near-bottom boundary layer cannot be resolved in case of poor vertical resolution in the model. Also, the theoretical values of the roughness parameters z_H and z_ξ (Voltsinger et al. 1989) are too small to play any significant role in experiments when the vertical grid step exceeds several metres.

A different approach is used to calculate the heat α_H and salt α_S coefficients of turbulent exchange. The following expression has been obtained (Kalatsky 1978):

$$\upsilon_H = \begin{cases} 0.0324\alpha_H l^2 D^{0.5} + \upsilon_0, & D \geq 0 \\ \upsilon_0, & D < 0 \end{cases} \qquad (16)$$

$$D = |\partial\bar{U}/\partial z|^2 + 0.067(\alpha_H T)/\partial z,$$

taking into account the possibility of generating an isothermal layer. To calculate the coefficient υ_S the term $-733.3\partial(\alpha_S S)/\partial z$ instead of $0.067\partial(\delta_H T)/\partial z$ is used (Kalatsky 1978). α_H and α_S are taken to equal to 0.1 (Kalatsky 1978).

At the horizontal walls the boundary conditions are adopted as the perfect insulation and slip for the velocity. For open boundaries we have used the tidal level oscillations (Proshutinsky 1993).

The zero velocities and undisturbed sea surface have been starting conditions. The initial salinity distribution has been vertically stable and horizontally homogeneous and during the experiment all the basin boundaries including open ones were closed for the salt exchange.

The discrete approximation of the model equations is given in (Polyakov et al. 1994).

The problem was solved numerically. A modelling area, developed by Proshutinsky (1993), includes the Arctic Ocean, the Greenland, Norwegian and Bartents seas (Fig. 1). The grid points have uniformly covered the domain with the step of 55.6 km. Nineteen vertical levels were used. The time steps were equal to 150 seconds and approximately 1.2 hour for the two- and three-dimensional blocks of the model. The latter time step has been taken for physical cause to resolve the tidal oscillations (it has been much smaller than a numerical stability criterion demands). The duration of the calculation was 250 tidal periods. The resulting salinity had oscillations within a tidal period, but being averaged

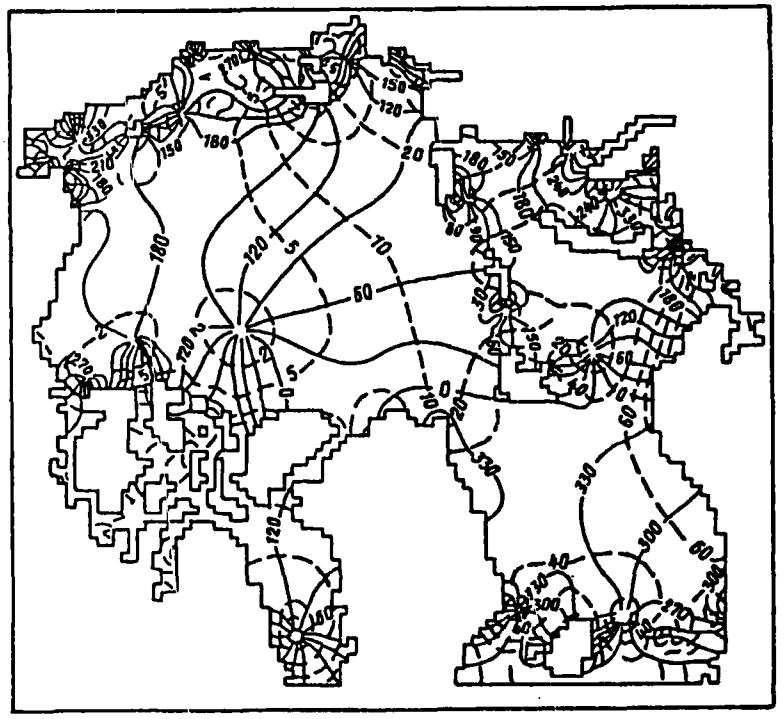

Fig. 2. Simulated tidal water level oscillations. Solid lines are isophases (degrees), dashed lines are isoamplitudes (cm).

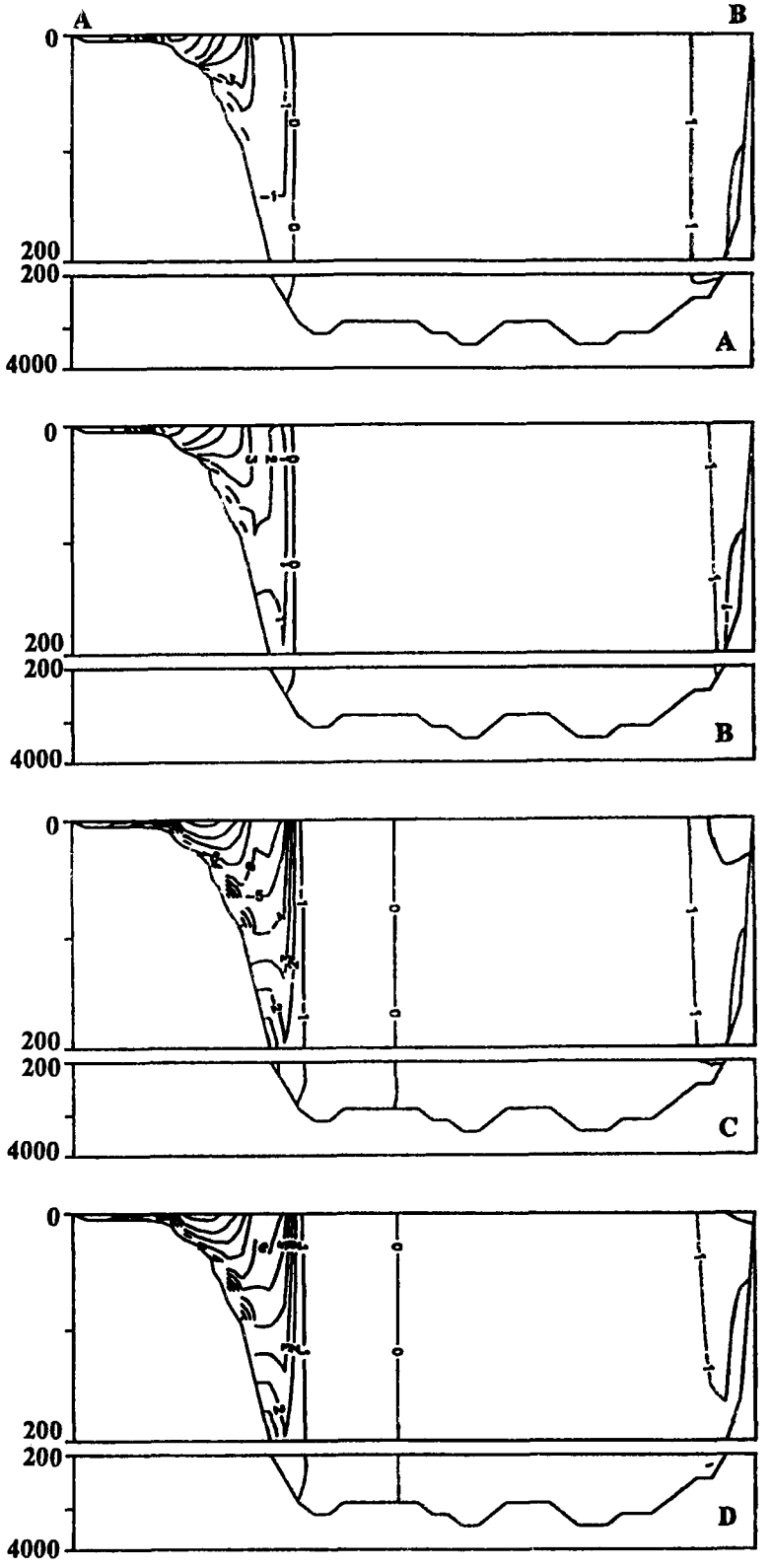

Fig. 3. Vertical cross-sections AB of two components U (A,B) and V (C,D) of the barotropic tidal current for opposite phases (A,C and B,D) of the tidal period (cm/s).

for the period, it was constant from one tidal period to another for every grid point.

Results

Simulation of the M2 tide in a barotropic Arctic Ocean

The simulated tidal level map is shown in Fig. 2. This scheme looks practically the same to that obtained, for instance by Proshutinsky (1993), with a two-dimensional model and with the same grid.

To validate the model results we have used the same sea level data of near-shore stations which were employed by Proshutinsky (1993). Correlation analysis of amplitudes and phases sets were carried out. The estimations are practically the same as those of Proshutinsky (1993). For example, the correlation coefficient between the calculated and observed amplitudes of the M2 tidal level oscillations is equal to 0.98.

The maximal velocities of the M2 tide are obtained at the boundary with the Atlantic Ocean, in the Baffin and Barents seas, on the shelves of the Laptev and East-Siberian seas. In the central part of the Arctic Ocean, tidal currents are small and do not exceed 1 cm/s. Unfortunately, we have no current data for the comparison. (The validation of the model by observed current data was carried out by Polyakov & Dmitriev (1993), while we used high spatial resolution of Baydatskaya Guba of the Kara Sea in the experiment).

The model has reproduced a 3D structure of the tidal flow. The vertical cross-sections of the simulated tidal current for the opposite phases of the tidal period are presented in Fig. 3. The position of the vertical cross-sections is shown in Fig. 1. The continental slope produces a relative separation of three areas with different dynamics of the tidal flow (Fig. 3). These areas comprise the shelf area which is significantly current-dependent on near-bottom boundary layer characteristics (Polyakov & Dmitriev 1993); the deep ocean area, where the tidal current is weak and vertically uniform; and the area of the continental slope with strong spatial variability and the most intensive dynamics of the tidal flow. The slope of the Laptev and New Siberian seas is marked out. Here the calculated surface velocity is about 20 cm/s, decreasing with depth of 1–2 cm/s. It is

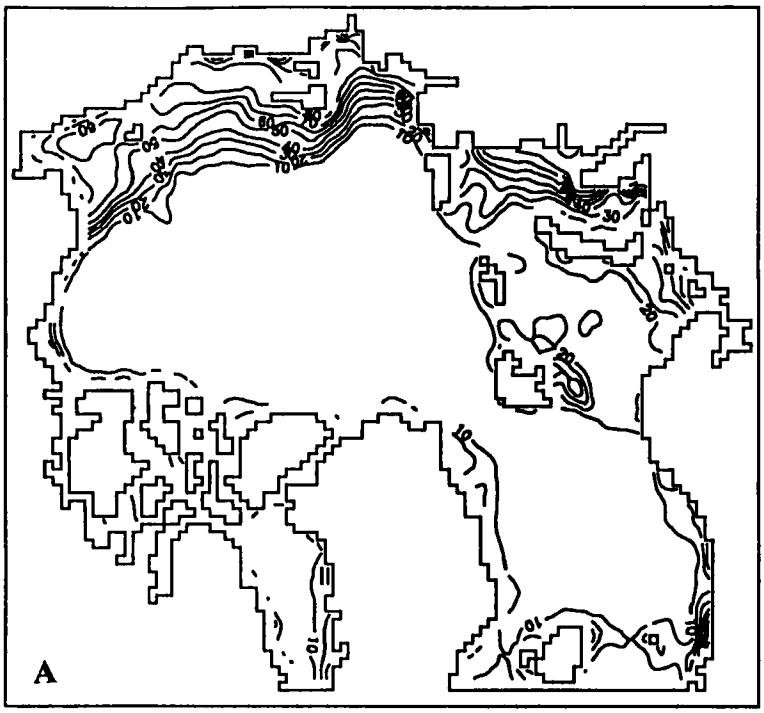

Fig. 4. Coefficients of the vertical turbulent exchange (cm/s) at levels 5 (A), 75 (B) and 500 (C) m.

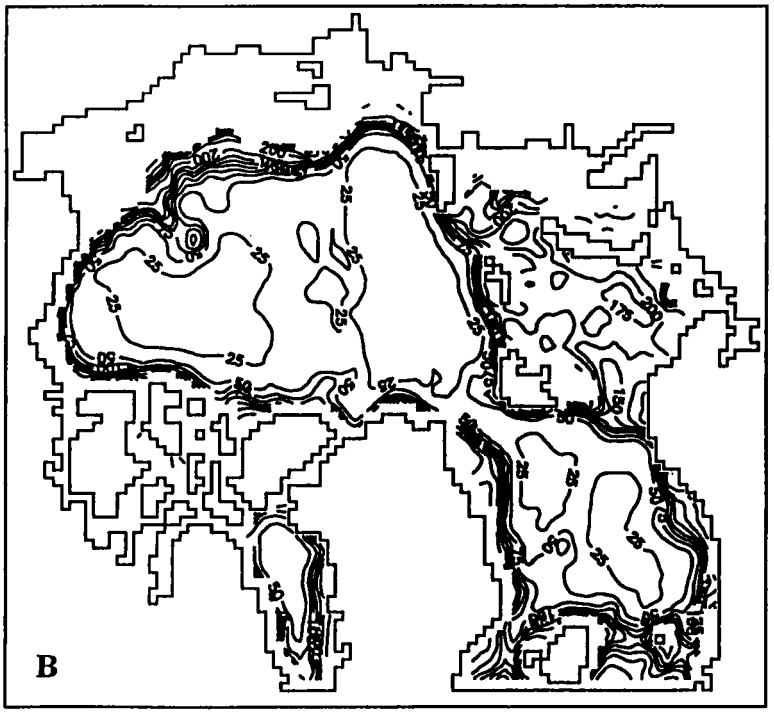
B

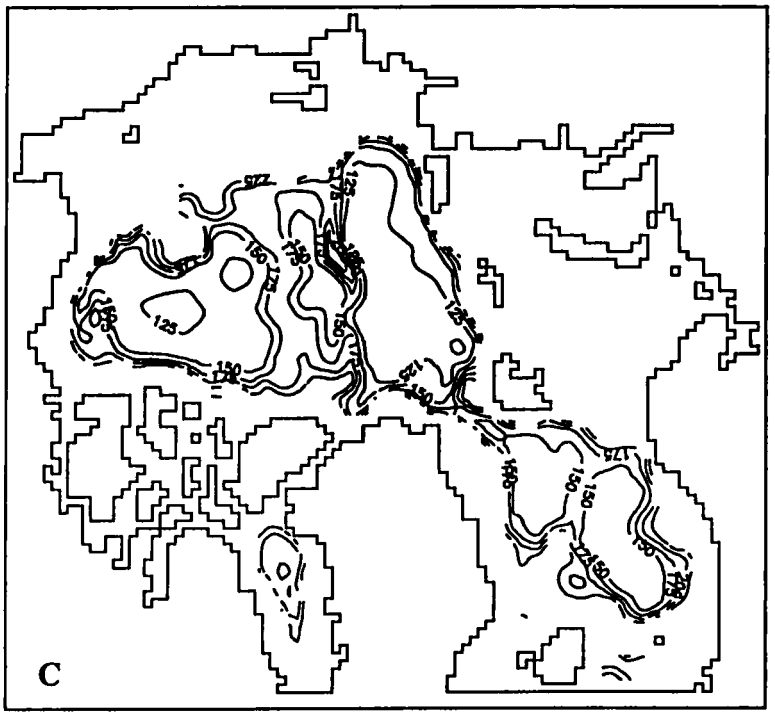
C

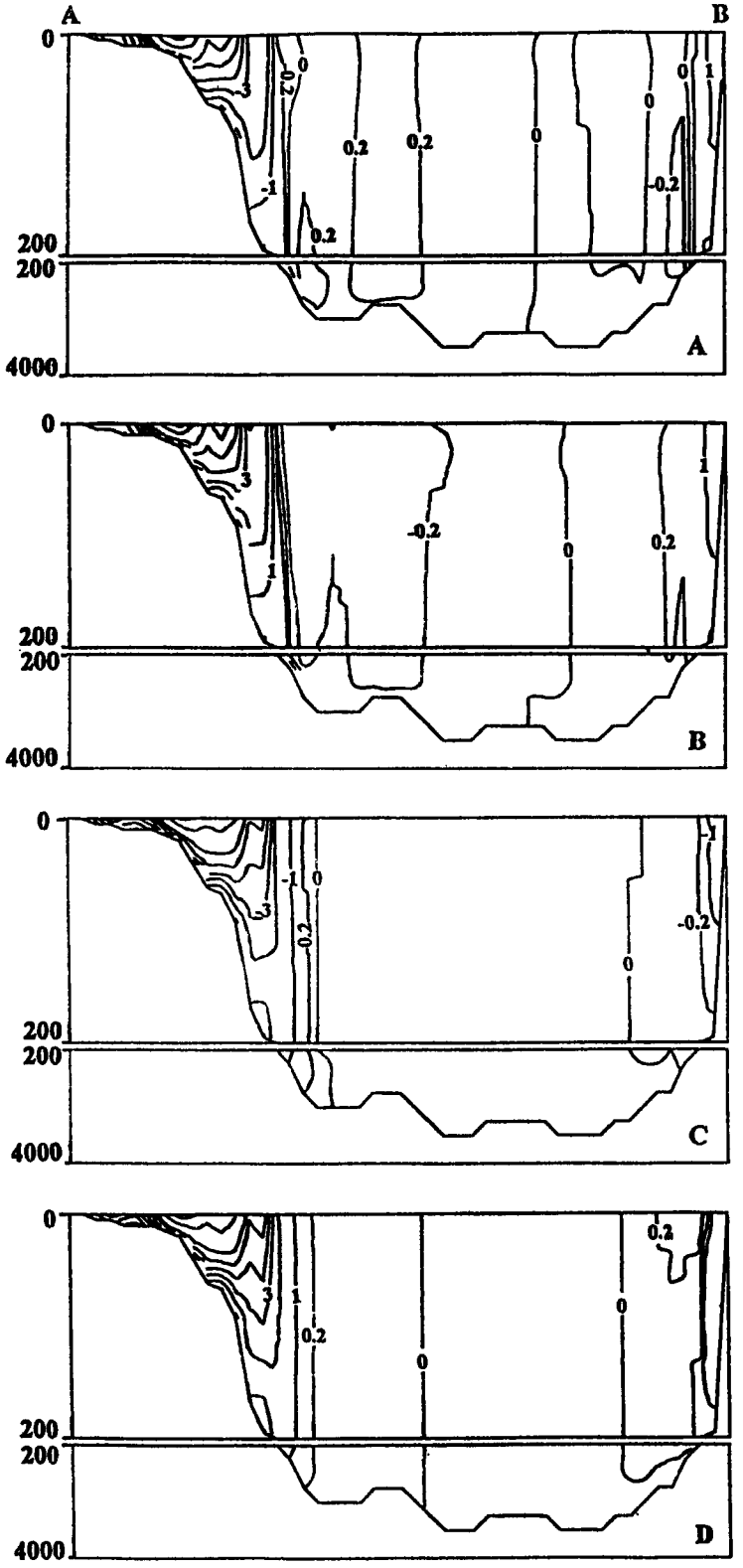

Fig. 5. The same as in Fig. 3, but for the baroclinic ocean.

important that in Fig. 3 one can observe a non-periodic component; in the case of absolutely periodical motion, the vertical cross-sections for opposite phases of the tidal period might be distinguished by sign only.

The calculated vertical viscosity coefficient υ_M for 5 m, 75 m and 500 m levels is shown in Fig. 4A, B and C. The values of the coefficient seem to be verisimilar and their spatial distribution is logical when the maximal values occur in areas with the most developed currents.

Simulation of the M2 tide in a baroclinic Arctic Ocean

Stratification has caused small variations in the structure of the tidal sea level. The statistical analysis of the 'barotropic' and 'baroclinic' fields shows that the coefficient of correlation is about 1 and the mean square roots of the sea level are 39.31 and 39.23 cm for each field. Maximal differences are concentrated in areas on the continental slope.

Baroclinicity was a cause for some rather small changes in the tidal currents; the density of the mean kinetic energy of currents was 1.2823 and 1.2796 KJ/m for the 'barotropic' and the 'baroclinic' problem, respectively. These changes led mainly to a weakening of the tidal currents. Velocity of the deep ocean decreased from approximately 0.5 to 0.35 cm/s. On the East-Siberian Sea slope the tidal current became weaker by about several cm/s. The vertical cross-section AB for the tidal currents in the case of the baroclinic Arctic Ocean is shown in Fig. 5. Baroclinic effects have also caused an intensification of the non-periodical component.

The tidal currents have been one reason for a reconstruction of the initial horizontally homogeneous salinity field (Fig. 6A and B). The resulting salinity is stable, i.e. the average over the tidal period solution was invariable in time.

It is important that the equations are non-linear. Indeed, had we integrated the linear equations for a long period, we should have obtained dissipation of the salinity gradients, i.e. the solution would be trivial. The application of the non-linear equations has enabled us to obtain another result when the balance between dynamical forcing and dissipation has been caused by the appearance of a stable structure (Schuster 1984).

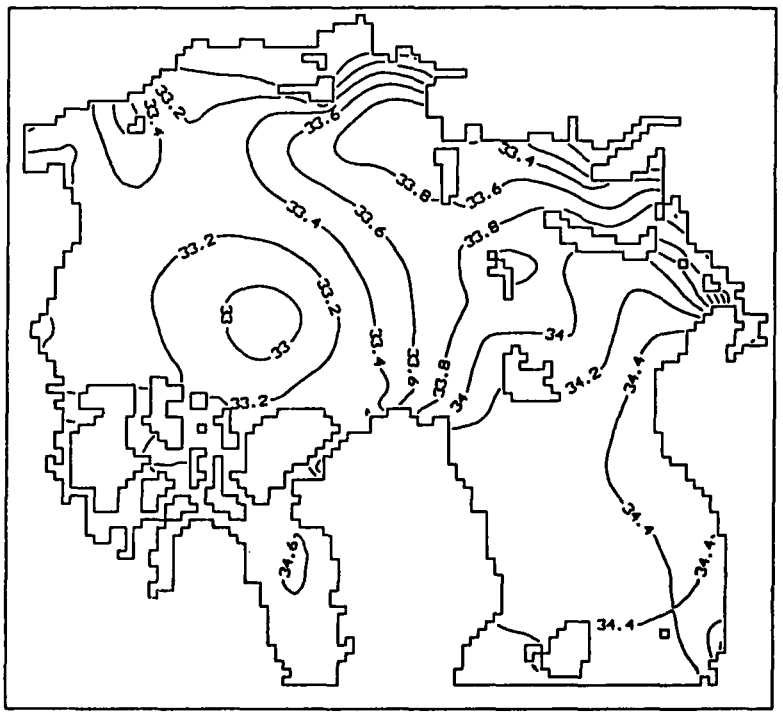

Fig. 6. Simulated salinity field at level 5 m.

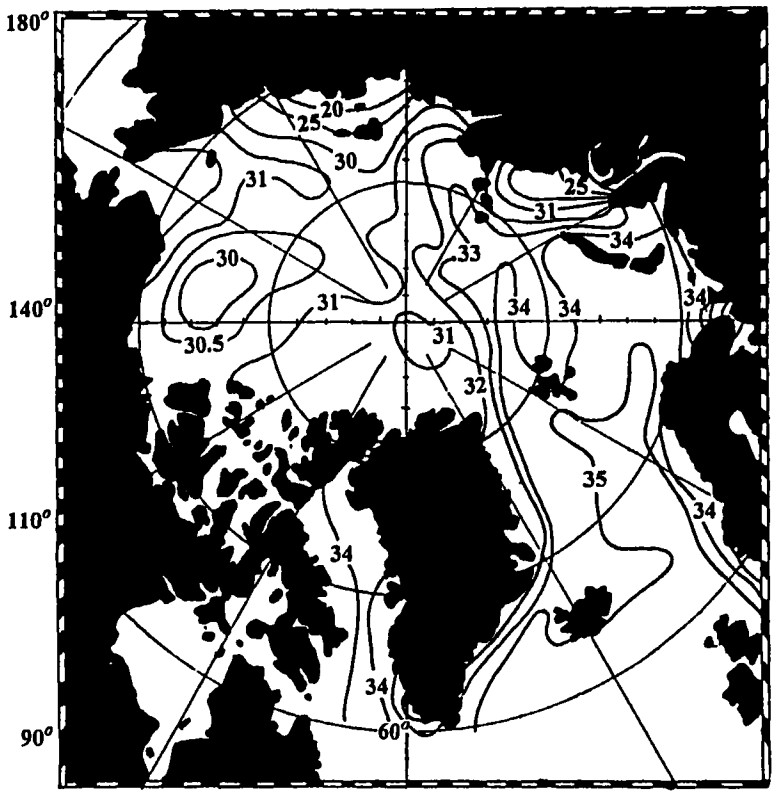

Fig. 7. Observed salinity field at level 5 m. (Gorshkov 1980).

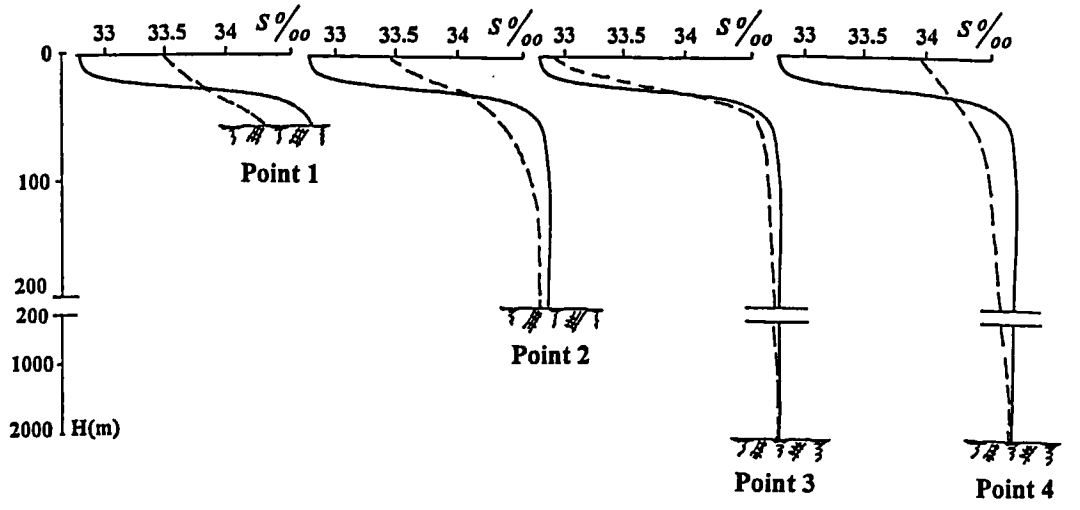

Fig. 8. Salinity profiles at points 1, 2, 3, 4 (Fig. 1). The solid lines denote the initial salinity profiles, the dashed ones present simulated profiles.

In this study we have not estimated the sensitivity of the system to its parameter variations, for example, to the initial vertical salinity distribution. This is a very important problem of the non-linear system sensitivity. Additional experiments are needed. At the same time, we suppose that the revealing of a stable regime of the system is in itself very important because it allows investigation of the mechanisms of the Arctic Ocean baroclinic fields formation.

We have compared the simulated and mean climatic salinity of the Arctic Ocean (Gorshkov 1980) (Figs. 6 and 7). These fields have many similar features. The 'river inflow' on the Siberian shelf, the high-gradient area in the shallows of the Barents Sea, and the 'tongue' of the saltwater penetrating from the Greenland Sea along the Lomonosov Ridge on to the Laptev Sea slope are well traced in Fig. 6. A surface salinity minimum was generated in the central part of the Arctic Ocean. It is changed by the salinity maximum at levels deeper than 75 m. The reason for such salinity redistribution is quite simple: weak tidal current in the central part of the Arctic Ocean has caused minimal erosion of the initial salinity profiles (Fig. 8). Intensive tidal motion at the Eurasian slope, near Iceland and the Lomonosov Ridge has produced more smoothed resulting salinity profiles.

This result will not seem to be so unexpected if we keep in mind that the Arctic Ocean bottom relief plays a very important, if nor crucial, role

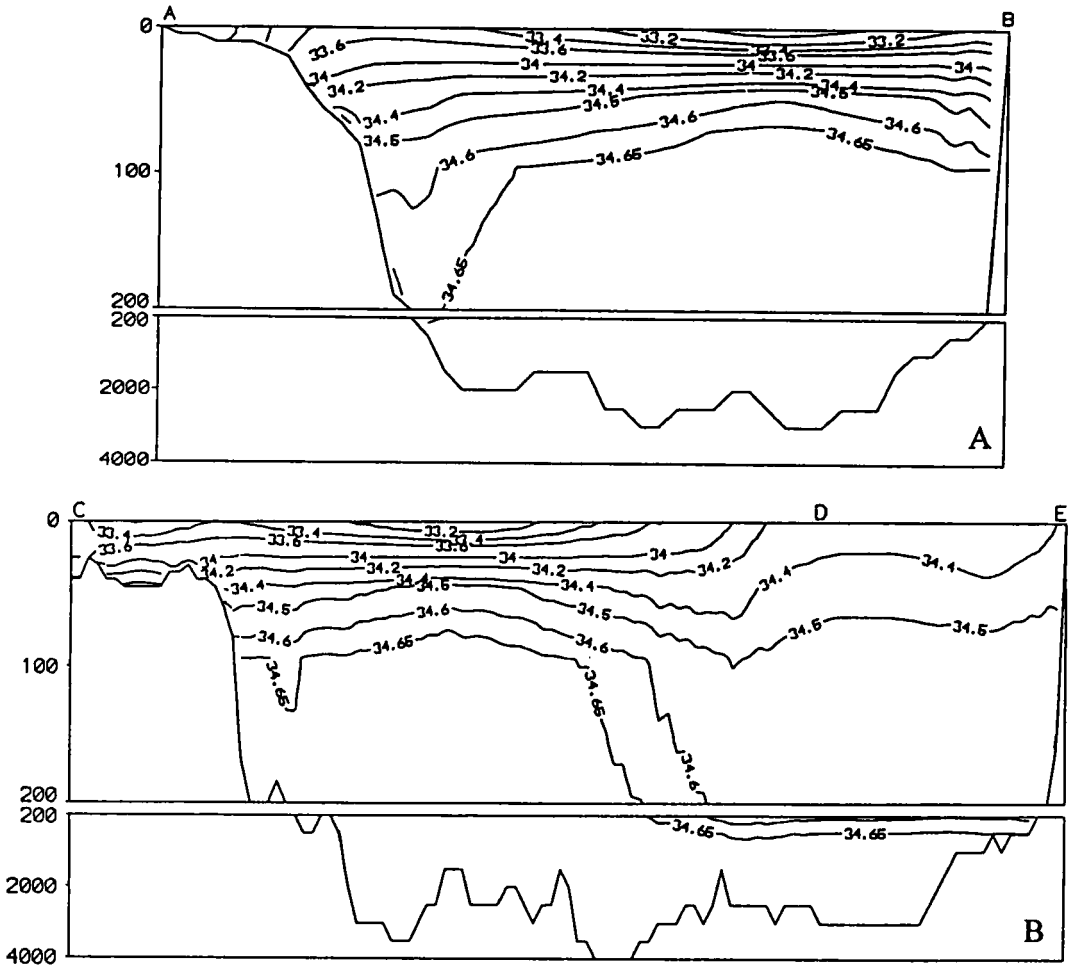

Fig. 9. Vertical cross-sections AB (A) and CDE (B) of the simulated salinity field.

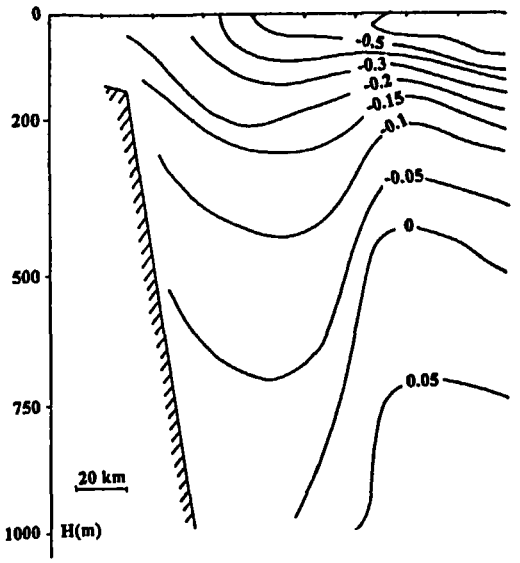

Fig. 10. Vertical cross-section of the observed density on the Laptev Sea continental slope. The values are in deviations from a mean value, a relative unit.

in the formation of the semidiurnal tides (Proshutinsky & Polyakov 1990). Thus in this experiment the salinity (density) field 'feels' the Arctic Ocean topography and the tidal dynamics is an intermediate point of this process. Therefore we conclude that some large-scale peculiarities of the baroclinic fields may be determined by the Arctic Ocean bottom relief.

One more interesting feature of the calculated salinity fields is the different distribution of the characteristics on continental slopes (Fig. 9). On the Greenland and the Chukchi sea slopes the resulting stratification is rather strong and it is weak at the slope of the Laptev (figure is not given) and East-Siberian Seas. The typical observed density distribution on the Laptev Sea slope (Fig. 10) is very similar to the calculated one. The salinity redistribution has been caused by the current of the semidiurnal tide M2, which itself is mainly determined by the topography of the ocean. Thus, peculiarities of continental slopes have had an influence on the salinity struc-

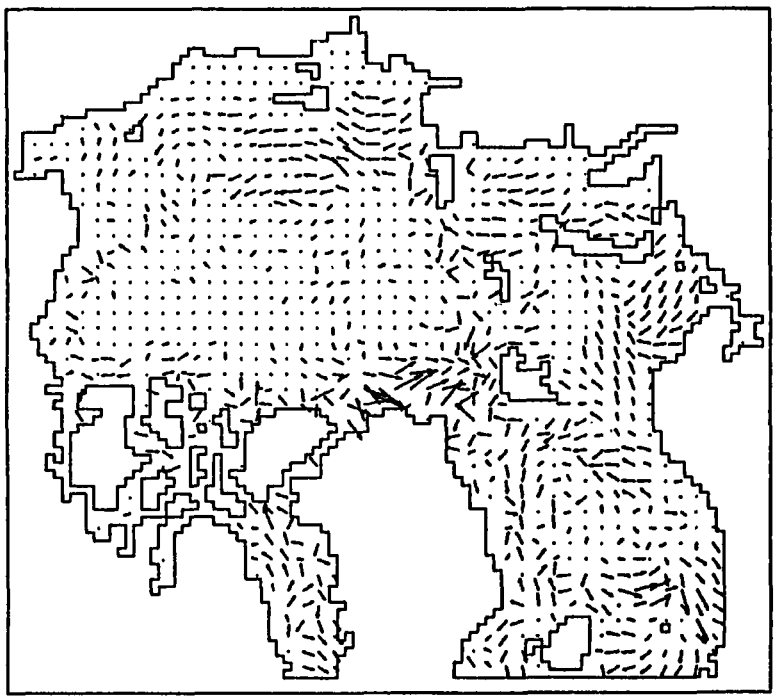

Fig. 11. Simulated baroclinic current at level 5 m. Arrows are plotted for every other grid point. The arrows are scaled using the maximal velocity value (about 7 cm/s).

ture on the different slopes. We suggest that tidal dynamics may be one reason for intensification of near-slope convection of the Laptev and East Siberian seas.

This conclusion is in good agreement with results of direct measurements of the Arctic Ocean water mass age: it is about 700 years old in the Canadian Basin and only about 30 years old in the Nansen Basin (Ostlund et al. 1987). Apparently, the bottom relief may determine the intensity of the near-slope convection of the Arctic Ocean.

Horizontal salinity gradients have caused stationary baroclinic circulation. The baroclinic flow at 5 m level is shown in Fig. 11. Weak density gradients have brought about very slow currents. For instance, current velocity does not exceed 0.01 cm/s in the central and near-shore parts of the ocean. Relatively large velocities (several cm/s) occur at the continental slopes of Greenland, the Laptev and East-Siberian seas.

The kinetic energy of this baroclinic current forms about 2% of the tidal expenditure on the bottom friction. Thus the maintenance of the stationary baroclinic circulation by the M2 tide is an additional sink of the barotropic tidal energy. The calculated kinetic energy of the density current may be a measure of this sink.

Conclusions

The M2 tidal level oscillations and 3D currents have been calculated for cases of the barotropic and baroclinic Arctic Ocean. The Arctic Ocean can be characterised by three regions: shallow water, slope regions, and the deep ocean area. The tidal dynamics of the shallow water area depends on characteristics of the near-bottom boundary layer. The continental slope regions have very intensive tidal currents with significant vertical variability. The tidal circulation of the deep ocean area is weak.

The baroclinicity is one reason for a weakening of the tidal currents and an intensification of its non-periodical component.

Due to tidal dynamics, the reconstruction of the initial horizontally homogeneous salinity distribution occurred. The resulting structure of the salinity field became stable in time which seems to be a property of a non-linear system behaviour.

The analysis of the calculated and observed mean climatic salinity fields has shown that these fields have similar features. We have connected this result with the importance of the Arctic Ocean bottom relief in the formation of the M2 tide which was the only forcing in the experiment. These facts have enabled us to conclude that some large-scale peculiarities of the baroclinic fields may be determined by the ocean topography.

It has been suggested that the tidal dynamics may be the cause of the intensification of near-slope convection of the Laptev and East-Siberian seas. This conclusion is based on an analysis of calculated vertical distribution of the salinity at different slopes. The weakest stratification produced by the M2 tide occurs on the slope of the Laptev and East-Siberian seas. In the observed salinity profiles of this area the penetration of light surface water into the deep layers also exists.

We have simulated baroclinic currents that correspond to the calculated density field of the ocean. The kinetic energy of this current may be a measure of an additional sink of the barotropic tidal energy.

Acknowledgements. – I would like to thank two anonymous reviewers for useful comments on the manuscript.

References

Aagaard, K. & Carmack E. C. 1989: The role of sea ice and other fresh water in the Arctic Ocean. *J. Geophys. Res. 94*, 14485–14498.

Blumberg, A. F. 1976: A Two-Dimensional Numerical Model for the Simulation of Partially Mixed Estuaries. Pp. 323–331 in Wiley, M. (ed.): *Estuarine Processes, Vol. 2.* Academic Press.

Blumberg, A. F. & Mellor, J. L. 1983: Diagnostic and prognostic numerical circulation studies of the South Atlantic Bight. *J. Geophys. Res. 88 (C8)*, 4579–4592.

Bryan, K. 1969: A numerical method for the study of the circulation of the World Ocean. *J. Comput. Phys. 4 (3)*, 347–376.

Caponi, E. A. 1976: The Simulation of Estuarine Circulation with a Fully Three-Dimensional Numerical Model. Pp. 332–346 in Wiley, M. (ed.): *Estuarine Processes, Vol. 2.* Academic Press.

Defant, A. 1924: Die Gezeiten des Atlantiscen Ozeans und des Arctischen Meeres. *Ann. Hydr. Marit. Met. Jahrg. (8–9)*, 153–166, 179–184.

Gjevik, K. B. & Straume, T. 1989: Model simulation of the M2 and K1 tide in the Nordic seas and the Arctic Ocean. *Tellus 41A*, 73–96.

Gorshkov, S. G. 1980: *Atlas of Oceans. Arctic Ocean.* 190 pp. (in Russian).

Hamilton, P. 1976: On the Numerical Formulation of a Time Dependent Multi-Level Model of an Estuary, with Particular Reference to Boundary Conditions. Pp. 347–364 in Wiley, M. (ed.): *Estuarine Processes. Vol. 2.* Academic Press.

Hendershott, M. C. 1977: Numerical models of ocean tides. Pp. 47–65 in: *The Sea.* Wiley Interscience, New York.

Johns, B. 1975: The form of the velocity profile in a turbulent shear wave boundary layer. *J. Geophys. Res. Vol. 80 (36)*, 5109–5112.

Johns, B. 1978: The modelling of tidal flow in channel using a turbulent energy closure scheme. *J. Phys. Oceanogr. 8 (5)*, 1042–1049.

Kagan, B. A. 1968: *Hydrodynamical models of the tidal motions in a sea*. Leningrad. HydroMeteoIzdat. 220 pp. (in Russian).

Kalatsky, V.I. 1978: *Modelling of the vertical thermal structure of the upper ocean layer*. Leningrad, HydroMeteoIzdat. 216 pp. (in Russian).

Killworth, P. D., Stamforth, B., Webb, B. J. & Paterson S. M. 1987: A free surface Bryan-Cox-Semtner model. *J. Phys. Oceanogr. 17 (7)*.

Kowalik, Z. 1981: A study of the M2 tide in the ice-covered Arctic Ocean. *Modeling, Identification and Control 1981, 2*, 201–223.

Kowalik, Z. & Proshutinsky, A. Yu. 1993: Diurnal Tides in the Arctic Ocean. *J. Geophys. Res. 98 (C9)*, 16449–16468.

Kowalik, Z. & Untersteiner, N. 1978: A study of the M2 tide in the Arctic Ocean. *Deutsche Hydr. Zeitsch. 31*, 216–229.

Leendertse, J. J. & Liu, S. K. 1977: A three-dimensional turbulent energy model for nonhomogeneous estuaries and coastal sea systems. Pp. 387–405 in Nihoul, J. J. (ed.): *Hydrodynamics of Estuaries and Fiords*. Proc. Ninth Int. Liege Colloq. Ocean Hydrodyn., Amsterdam. Elsevier Scientific Publ., New York.

Liu, S. K. & Leendertse, J. J. 1979: *A Three-Dimensional Model for Estuaries and Coastal Seas. Vol. 6. Bristol Bay Simulations*. RAND, R-2405-NOAA. 121 pp.

Liu, S. K. & Leendertse, J. J. 1987: *Modeling the Alaskan Continental Shelf Waters*. Oct. 1987, R-3567-NOAA/RC RAND Corporation. 136 pp.

Oey, L.-Y., Mellor, G. L. & Hires, R. I. 1985: A three-dimensional simulation of the Hudson-Raritan Estuary. Part 1: Description of the model and model simulation. *J. Phys. Oceanogr. 15 (12)*, 1676–1692.

Ostlund, H. G., Possnert, G. & Swift, J. H. 1987: Ventilation rate of the deep Arctic Ocean from carbon 14 data. *J. Geophys. Res. 92*, 3769–3777.

Polyakov, I. V., Dmitriev, N. E. 1993: Modelling of the vertical structure of the storm surges and tides of a shallow-water basin. *Meteorologiya i gydrologiya 12*, 54–62. (in Russian)

Polyakov, I. V., Kulakov, I. Yu., Kolesov, S. A., Naumov, A. K., Dmitriev N. Eu. 1994: Coupled ice-ocean dynamics model of the Kara Sea. Tech. Report N 4-YA-94. AARI, St. Petersburg, Russia. 194 pp.

Proshutinsky, A. Yu. 1993: *The Arctic Ocean level oscillations*. St. Petersburg, HydroMeteoIzdat. 216 pp. (in Russian)

Proshutinsky, A. Yu & Polyakov, I. V. 1990: The Arctic Ocean Eigen Oscillations. *Proceedings of An Intern. Conf. on the Role of the Polar Regions in Global Change, June 11–15 1990*. Univ. Alaska, Fairbanks. Pp. 347–354.

Schuster, H. G. 1984: *Deterministic Chaos. An Introduction*. Physik-Verlag, Weinheim.

Semtner, A. J. Jr. 1974: An oceanic general circulation model with bottom topography. Tech. Report N 9. Department of Meteorology University of California. USA. 99 pp.

Schwiderski, E. W. 1980: Ocean tides. Part II: A hydrodynamical interpolation model. *Marine Geodesy 3*, 219–255.

Voltsinger, N. E., Klevanny, K. A. & Pelinovsky E. N. 1989: *Long-wave dynamics of the near-shore zone*. Leningrad, HydroMeteoIzdat. 272 pp. (in Russian)